*Thermochimica Acta*, 78 (1984) 251–260
Elsevier Science Publishers B.V., Amsterdam – Printed in The Netherlands



# THE THERMAL STABILITY OF BINARY ALKALI METAL NITRATES

OSAMI ABE *, TAIZO UTSUNOMIYA and YOSHIO HOSHINO

*Research Laboratory of Engineering Materials, Tokyo Institute of Technology, Nagatsuta, Midori-ku, Yokohama, 227 (Japan)*

(Received 17 February 1984)

## ABSTRACT

The thermal stability of binary alkali metal nitrates has been investigated by DSC and the simultaneous measurement of TG, DTA, DTG and EGA. The solid solutions containing sodium nitrate are thermally unstable and cluster readily to each component species. The decomposition temperature of nitrates does not decrease by the coexistence of other nitrates, while the melting temperature does decrease. The behavior of the thermal decomposition is reasonably interpreted by thermodynamic considerations.

## INTRODUCTION

Fused alkali metal nitrates and their liquid mixtures are of interest as heat storage materials and reaction media as well as the melts of nitrate–hydroxide and hydroxide–hydroxide systems [1–4]. Properties relating to the melts such as mobility of cations, EMF data and surface tension have been investigated extensively [5–10]. The thermal decomposition of pure nitrates and the reaction of nitrates with several oxides were investigated and information on the reactivity of nitrate melts was obtained previously [11–14]. The phase diagram and thermodynamic properties of $NaNO_3$–$KNO_3$ system have been reconsidered with up-to-date machines and analytical techniques for thermal analysis [15,16]. Few studies, however, have been made in this field for other nitrate systems.

The present paper deals with the thermal stability of solid and liquid solutions of the binary systems of $NaNO_3$ with other alkali metal nitrates. The phase diagrams were constructed by DSC for the thermodynamic consideration. The thermal decomposition of the binary melts was investigated by the simultaneous measurement of TG, DTA, DTG and EGA.

* Present address: Government Industrial Research Institute, Nagoya, 1 Hirate-cho, Kita-ku, Nagoya, 462, Japan.

0040-6031/84/$03.00 

## EXPERIMENTAL

### *Materials*

Reagent grade $LiNO_3$, $NaNO_3$, $KNO_3$ and $CsNO_3$ (Wako Pure Chemicals) were ground to below 100 mesh, dried at 200 °C for 50 h and stored in a glove box filled with dry argon. Silica ($\alpha$-quartz; Kyoritsu Yogyo Genryo) was ground to below 100 mesh by a ball mill, washed with nitric acid (0.1 mol $l^{-3}$) and redistilled water and dried at 105 °C. These chemicals were mixed by dry blending in the glove box. Silica was added to the salt mixtures for measurement of the thermal decomposition.

### *Apparatus and procedure*

The DSC measurement was carried out with a Rigaku Denki TG–DSC apparatus. The calibration of the apparatus was made by high purity In, Sn and Pb as standard samples. The salt mixture in a platinum vessel (10 mg) was held at 200 °C for 1 h in the apparatus to remove adsorbed water and heated several times in an atmosphere of dry argon at a rate of 5 °C $min^{-1}$.

The simultaneous measurement of TG, DTA, DTG and EGA was performed with a Rigaku Denki TG–DTA unit, a Rika Denki Kogyo differentiator, and a Simadzu Seisakusyo gas chromatograph. The samples were heated at a rate of 5 °C $min^{-1}$ in an atmosphere of dry argon (flow rate: 50 $cm^3$ $min^{-1}$) after the heat treatment at 200 °C for 1 h. The decomposition gas was introduced into the gas chromatograph every 2 min by an auto gas sampler. The details of the measurement have been discussed previously [11,12].

## RESULTS AND DISCUSSION

### *DSC measurement and phase diagrams*

Figure 1 shows the DSC profiles for the salt mixtures of the $NaNO_3$–$KNO_3$ system. The heating rate (1.25 to 10 °C $min^{-1}$), the sample weight (2–20 mg) and the atmosphere (air or argon) negligibly affect the DSC profiles. The salt mixtures did not decompose during the DSC measurement because the weight loss was negligibly small (within 0.1 wt% of the dried sample). From the result of the chemical analysis of the vessels, no reaction occurred between the salt mixtures and the vessels. The DSC profile of the 1 : 1 mixture (mole fraction of $NaNO_3$, $\chi = 0.50$) shows that typical of the eutectic mixture. To determine the eutectic composition, the sharpness of the DSC peaks (expressed by the ratio of peak height to half the width) was compared from sample to sample in the composition range $\chi = 0.45$–$0.50$ at

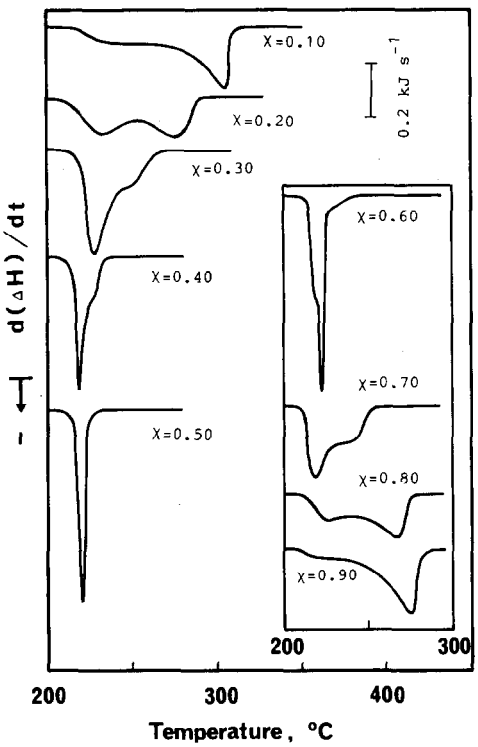


Fig. 1. DSC profiles of the mixture of $NaNO_3$ and $KNO_3$. Heating rate, 5 °C $min^{-1}$; atmosphere, Ar (50 $cm^3$ $min^{-1}$); sample weight, 10 mg. The molar fraction of $NaNO_3$ is indicated by $\chi$.

0.01 intervals. The sharpest peak was observed for the sample of $\chi = 0.53$. The eutectic temperature was determined from the heating and cooling profiles of this composition (see Fig. 2). The solidus and liquidus temperatures were decided from the lowest and highest temperature deviations from the base lines of the DSC profiles.

The phase diagram obtained is shown in Fig. 3 for the $NaNO_3$–$KNO_3$ system. The liquidus temperatures are slightly lower than those calculated by Kramer and Wilson's [15] method, but quite close to those by Kofler [17]. The flat solidus was obtained in the composition range 0.10–0.90. The solidus temperatures were extremely close to the temperatures reported by Kramer and Wilson [15]. The DSC peaks of the solid-state transformation of $NaNO_3$ (275 °C, ordered rhombohedral to disordered rhombohedral) and $KNO_3$ (128 °C, orthorhombic to rhombohedral) were not observed, but quite small peaks were observed at 120 °C. This suggests that relatively stable solid solutions are formed in this system.

The crystal structures of $LiNO_3$, $NaNO_3$, $KNO_3$ and $RbNO_3$ are trigonal just below the melting point, while $CsNO_3$ is cubic. The limited solid solution may be formed in the binary system of $NaNO_3$ and $CsNO_3$ which

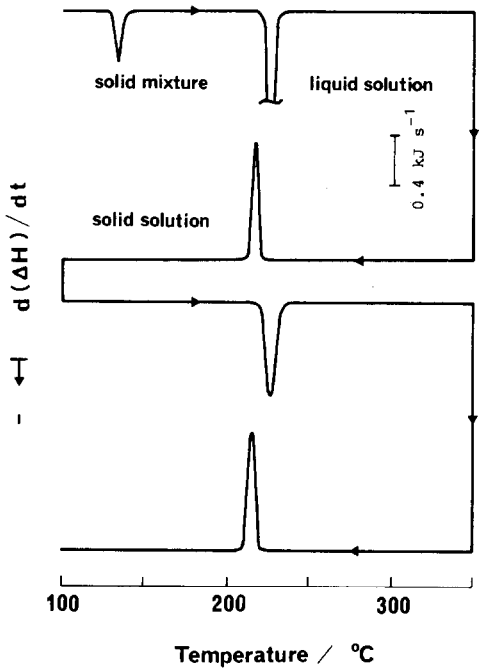


Fig. 2. DSC profiles of the sample with eutectic composition ($\chi = 0.53$) in the $NaNO_3$–$KNO_3$ system.

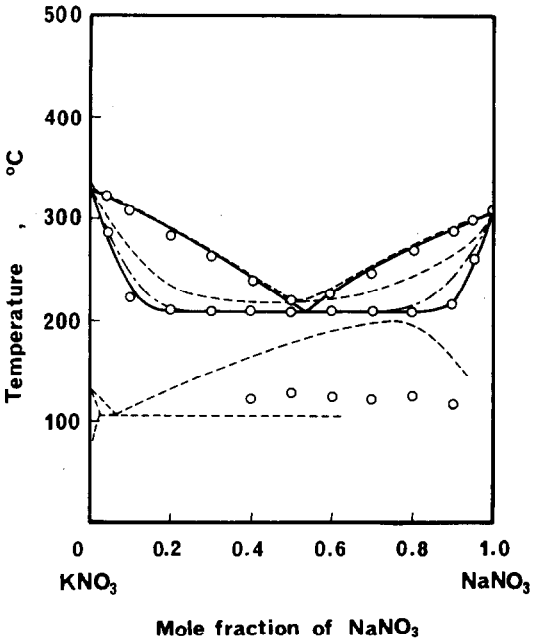


Fig. 3. Phase diagram of the $NaNO_3$–$KNO_3$ system. (———) Present study; (— — —) Kofler [17]; (·–·–·) after calculation by Kramer's method.

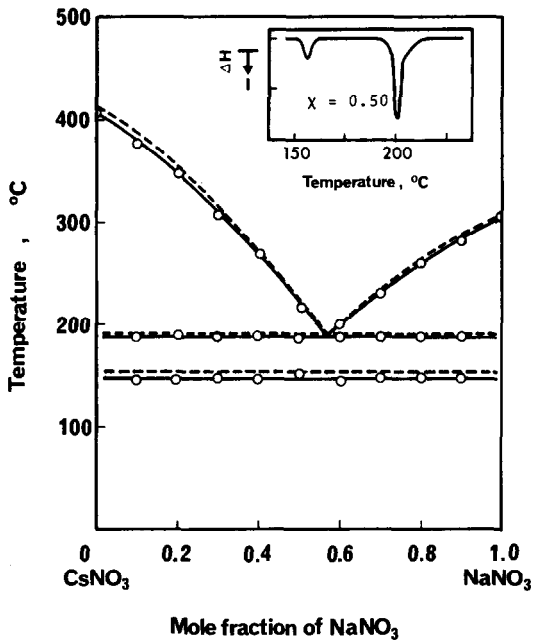


Fig. 4. Phase diagram of the $NaNO_3$–$CsNO_3$ system and a typical DSC profile. (——) Present study; (— — —) Bol'shakov [18].

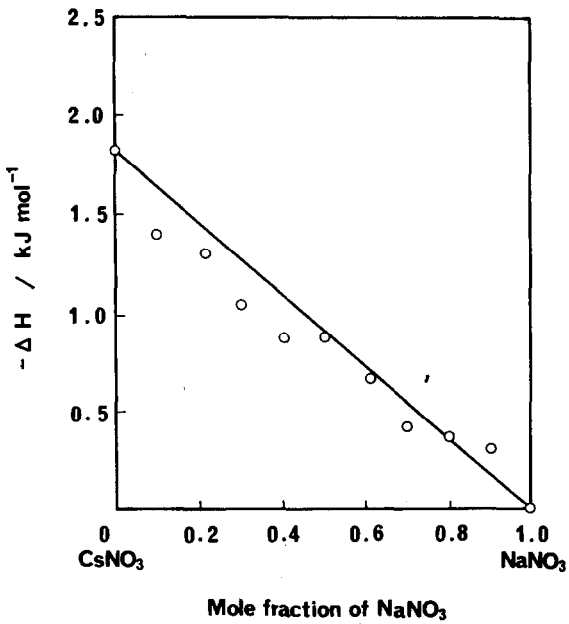


Fig. 5. Heat of transformation of the $NaNO_3$–$CsNO_3$ system as a function of $NaNO_3$ content.

belongs to a different crystal system. Figure 4 shows the phase diagram and a typical DSC profile ($\chi = 0.50$) for the $NaNO_3$–$CsNO_3$ system. The solidus and liquidus temperatures and the eutectic composition were determined by the same procedures as for the $NaNO_3$–$KNO_3$ system. The eutectic composition was $\chi = 0.57$. The obtained phase diagram agreed well with that reported by Bol'shakov et al. [18].

Endothermic peaks were observed around 150 °C in DSC profiles for the samples containing $CsNO_3$ irrespective of their composition. According to Pashin and Radonchie [19], the transformation of hexagonal $\beta$-$RbNO_3$ to cubic $\gamma$-$RbNO_3$ takes place around 160 °C in the $NaNO_3$–$RbNO_3$ system, which forms the limited solid solution. This suggests that the endothermic peak is caused by the solid-state transformation of $CsNO_3$. The heat of transformation was plotted against the molar fraction of $NaNO_3$ ($\chi$). The result is shown in Fig. 5. The heat of transformation is linearly related to the content of cesium salt in the samples. This indicates that the interaction of like ions is larger than that of unlike ions, when the solid solution is thermally unstable. The limited solid solution should be formed in the $NaNO_3$–$CsNO_3$ system.

*Thermal stability of solid solutions*

The solid solutions between $NaNO_3$ and other alkali metal nitrates were unstable at room temperatures because X-ray diffraction patterns of quenched samples showed the mixture of each component. The enthalpy of mixing obtained from the regular solution theory will form part of the basis to estimate the thermal stability of solid solutions. Kramer and Wilson [15] indicated the regular solution theory to be applicable to the calculation of solidus and liquidus temperatures of the $NaNO_3$–$KNO_3$ system. They used Kleppa's data for liquid solutions [20], where the enthalpy and entropy of mixing ($\Delta H^s_{mix}$ and $\Delta S^s_{mix}$) were expressed by the following equations

$$\Delta H^s_{mix} = 6.28\chi(1-\chi) \tag{1}$$

$$\Delta S^s_{mix} = -R[\chi \ln \chi + (1-\chi) \ln(1-\chi)] \tag{2}$$

where $\chi$ = molar fraction of $NaNO_3$, $R$ = gas constant.

The free energy of mixing was calculated to be $-1.24$ kJ mol$^{-1}$ for the solid solution of $\chi = 0.50$ at the solidus temperature (215 °C). Therefore, the solid solution is thermally stable at the solidus temperature, although the positive enthalpy ($\Delta H^s_{mix} = 1.57$ kJ mol$^{-1}$ at $\chi = 0.50$) indicates that the solid solution has a tendency toward clustering to each constituent species.

The regular solution approximation is not applicable to the systems forming limited solid solutions. For the present case, the enthalpy of mixing can be obtained from the equilibrium distribution coefficient of impurity nitrates to the host crystal ($NaNO_3$, in the present case) according to the

dilute solution theory. The enthalpy and entropy of mixing has been previously estimated [21] by using equilibrium distribution coefficients ($k$) and the literature values of enthalpy and entropy of fusion of the host crystal for the binary alkali metal nitrate systems containing $NaNO_3$. The maximum enthalpy of mixing ($\Delta H^s$) calculated by eqn. (3) are listed in the 3rd column on Table 1.

$$\Delta H^s = \Delta H^f(NaNO_3) - T\Delta S^f(NaNO_3) - RT \ln k \quad (3)$$

where $\Delta H^f$ = enthalpy of fusion of host crystal, $\Delta S^f$ = entropy of fusion of host crystal, $k$ = equilibrium distribution coefficient, $T$ = solidus temperature.

The calculated maximum enthalpy for the $NaNO_3$–$KNO_3$ system by eqn. (3) (1.34 kJ $mol^{-1}$) agrees well with the maximum enthalpy by eqn. (1) (1.57 kJ $mol^{-1}$). The free energy of mixing is calculated to be 0.06, −1.29, 1.64 and 5.27 kJ $mol^{-1}$ for the solid solutions of the systems $NaNO_3$–$LiNO_3$, –$KNO_3$, –$RbNO_3$ and –$CsNO_3$, respectively, at the solidus temperatures and the composition $\chi = 0.50$. As the enthalpy and free energy of mixing increase, the solid solution becomes thermally unstable and tends to cluster to like ions. This results in a phase separation to each component salt. Therefore, the $NaNO_3$–$KNO_3$ system forms the most thermally stable solid solution and the $NaNO_3$–$CsNO_3$ solid solution shows a phase separation. These thermodynamic considerations are in agreement with the results of the DSC measurement and X-ray diffractometry in the discussion on the phase diagrams.

*Thermal stability of liquid solutions*

The regular solution theory is also applicable to the estimation of the thermal stability of liquid solutions. Kleppa derived the following relation with respect to the enthalpy of mixing ($\Delta H^l_{mix}$) for the liquid solutions of the

TABLE 1

Maximum enthalpy of mixing of solid and liquid solutions in the $NaNO_3$–$MNO_3$ system

| M | Pauling's ionic radius of M (nm) | Maximum enthalpy of mixing [a] (kJ $mol^{-1}$) | |
|---|---|---|---|
| | | Solid solution | Liquid solution |
| Li | 0.060 | 2.72 | −0.632 |
| K | 0.133 | 1.34 | −0.576 |
| Rb | 0.148 | 4.30 | −1.07 |
| Cs | 0.169 | 7.93 | −2.08 |

[a] The values are calculated by the following equations for the solutions with the composition of $\chi = 0.50$: solid solution, $\Delta H^s_{mix} = \Delta H^f(NaNO_3) - \Delta S^s(NaNO_3) - RT \ln k$; liquid solution, $\Delta H^l_{mix} = -586\chi(1-\chi)\delta^2$.

$NaNO_3$–$KNO_3$ system by a calorimetric method [20]

$$\Delta H^1_{mix} = \chi(1-\chi)(-1.71-0.28\chi) \quad (4)$$

where $\chi$ is the molar fraction of $NaNO_3$. Negative values of the enthalpy are obtained from eqn. (4) in the whole composition range.

On the other hand, the enthalpy of mixing for liquid solutions of the binary alkali metal nitrate systems is related to the ionic radii of the component species by the following equations [22]

$$\Delta H^1_{mix} = -586\chi(1-\chi)\delta^2 \quad (5)$$

where $\delta$ is the size parameter expressed by

$$\delta = (r_1 - r_2)/(r_1 + r_2 + 2r_-) \quad (6)$$

where $r_1$, $r_2$ = Pauling's ionic radii of cations; $r_-$ = anion radius.

The maximum enthalpy of mixing calculated by eqns. (5) and (6) is listed in the 4th column of Table 1. The thermodynamic radius of 0.187 nm was used for the calculation as the radius of the nitrate anion ($r_-$).

The maximum enthalpy of mixing obtained by eqns. (4) and (5) is $-0.463$ and $-0.576$ kJ mol$^{-1}$, respectively. The difference between the two values is not significant for discussion because it is within 0.25 of the smallest value in Table 1.

Negative enthalpy is obtained for the liquid solutions of all the systems discussed in the present paper. The maximum enthalpy is quite small in the two systems $NaNO_3$–$LiNO_3$ and $NaNO_3$–$KNO_3$, and indicates that the solutions have approximately the same characteristics as the ideal solutions. Relatively large negative values of the maximum enthalpy in the systems $NaNO_3$–$RbNO_3$ and $NaNO_3$–$CsNO_3$ indicate the relatively large interaction between the unlike ions in the liquid solutions.

The calculated free energy of mixing of the 1 : 1 mixture is $-7.24$, $-7.18$, $-7.68$ and $-8.69$ kJ mol$^{-1}$ for the liquid solutions of $NaNO_3$–$LiNO_3$, –$KNO_3$, –$RbNO_3$ and –$CsNO_3$ at 300 °C, respectively. The contribution of the entropy term to the free energy is 91, 92, 86 and 76%, respectively. The contribution increases to 93, 94, 89 and 81% at 500 °C, respectively. These liquid solutions are supposed to be random solutions because the free energy of mixing strongly depends on the entropy term. It may be easily assumed that the thermal decomposition of a component proceeds independently, irrespective of the coexistence of other salt components in these liquid solutions.

Figure 6 shows the EGA curves during the course of the thermal decomposition of $NaNO_3$, $KNO_3$ and their mixture ($\chi = 0.50$). The decomposition mechanism of pure nitrates has been discussed previously [11–14]. The decomposition temperatures of $NaNO_3$ and $KNO_3$ did not decrease by the coexistence of other nitrates ($KNO_3$ and $NaNO_3$, respectively), while the melting temperatures decreased (see Fig. 1). It is evident from Fig. 6 that the

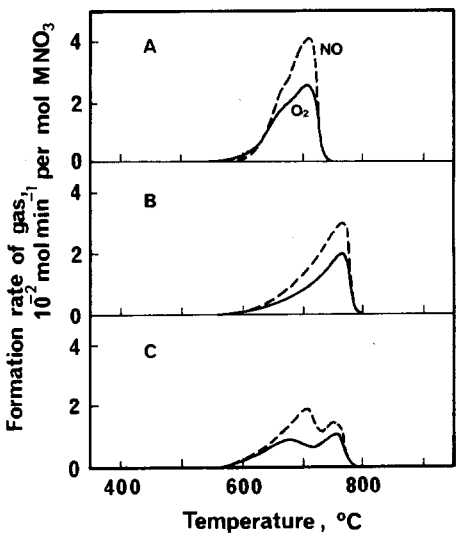


Fig. 6. EGA curves of the thermal decomposition of $NaNO_3$ (A), $KNO_3$ (B), and the mixture of $NaNO_3$ ($\chi = 0.50$) and $KNO_3$ (C). Heating rate, 5 °C $min^{-1}$; atmosphere, Ar (50 $cm^3$ $min^{-1}$); samples contain 0.2 mmol nitrates.

EGA curves for the mixture of the $NaNO_3$–$KNO_3$ system ($\chi = 0.50$) have two peaks and each peak corresponds to the thermal decomposition of pure nitrates. Potassium nitrate was identified by X-ray diffractometry of the quenched sample of $\chi = 0.50$ from 750 °C, while $NaNO_3$ was not detected in the sample. The weight loss of the first step of the decomposition ( < 725 °C) was 50.6% of the final weight loss. The ratio of the amount of formed $O_2$ to NO were 0.78 and 0.73 below and above 725 °C, respectively. These facts, as is expected by the thermodynamic consideration, indicate that the thermal decomposition of $NaNO_3$ takes place independently to that of $KNO_3$.

The maximum enthalpy of mixing for the liquid solutions decreases as the difference between the cation radii of the component species increases, while that of the solid solutions increases. This indicates that the stability increases in liquid solutions with increasing difference, while that in solid solutions decreases. These thermodynamic considerations have been confirmed by the DSC measurement and the thermal analysis of the decomposition.

## REFERENCES

1 Y. Takahashi, M. Kamimoto, T. Ozawa, R. Sakamoto and Y. Abe, 1st Symp. Molten Salt Chem. Technol., Kyoto, 1983, pp. 1–313.
2 Y. Takahashi, M. Kamimoto, R. Sakamoto, K. Kanai and T. Ozawa, Nippon Kagaku Kaishi, (1982) 1049.
3 S.K. Jain and H.C. Gaur, J. Indian Chem. Soc., 54 (1977) 618.
4 M. Kosaka, T. Asahina, H. Taoda and A. Kishi, Nippon Kagaku Kaishi, (1982) 977.

5 I. Okada and R. Takagi, Z. Naturforsch., Teil A, 34 (1979) 498.
6 M. Okada and K. Kawamura, Electrochim. Acta, 15 (1970) 1.
7 M. Okada and K. Kawamura, Electrochim. Acta, 19 (1974) 777.
8 M.M. Abraham and M.C. Trudelle, J. Chim. Phys., 73 (1976) 863.
9 M.M. Abraham and M.C. Trudelle, J. Chim. Phys., 74 (1977) 638.
10 H. Bloom, F.G. Davis and D.W. James, Trans. Faraday Soc., 56 (1960) 1179.
11 Y. Hoshino, T. Utsunomiya, T. Utsugi and O. Abe, Nippon Kagaku Kaishi, (1980) 690.
12 Y. Hoshino, T. Utsunomiya and O. Abe, Bull. Chem. Soc. Jpn., 54 (1981) 1385.
13 O. Abe, T. Utsunomiya and Y. Hoshino, Bull. Chem. Soc. Jpn., 56 (1983) 428.
14 O. Abe, T. Utsunomiya and Y. Hoshino, Thermochim. Acta, 74 (1984) 131.
15 C.M. Kramer and C.J. Wilson, Thermochim. Acta, 42 (1980) 253.
16 D.J. Rogers and G.J. Jantz, J. Chem. Eng. Data, 28 (1983) 201.
17 A. Kofler, Monatsh. Chem., 86 (1955) 646.
18 K.A. Bol'shakov, B.I. Pokrovskii and V.E. Plyshchev, Zh. Neorg. Khim., 6 (1961) 2120.
19 N.A. Pashin and M. Radonchie, Glas. Hem. Drus. Kralj. Jugosl., 6 (1937) Sect. 8, 25.
20 O.J. Kleppa, J. Phys. Chem., 64 (1970) 1937.
21 T. Utsunomiya and Y. Hoshino, 48th Annu. Meet. Chem. Soc. Jpn., Preprint I, p. 56, August 1983.
22 O.J. Kleppa and L.S. Hersh, J. Chem. Phys., 34 (1961) 351.